

Inverse photoconductivity effect in triple cation organic-inorganic hybrid perovskite memristors with various iodine concentrations, electrodes, and modified layers

Yucheng Wang¹, Yuxuan Xiong¹, Jian Sha¹, Jiyang Guo¹, Hongsu Wang¹, Ziqing Qiang¹, Yueyang Shang¹, Renxu Jia², Kai Sun², Fobao Huang¹, Xuetao Gan¹ and Shaoxi Wang^{1*}

¹School of Microelectronics, Northwestern Polytechnical University, Xi'an, 710072, China

²School of Microelectronics, Xidian University, Xi'an, 710072, China

*Email: shxwang@nwpu.edu.cn

UV-vis absorption spectrum of the perovskite is shown in Fig. S1a. It is clearly seen that the perovskite layer can absorb in the range of most visible light. ***In addition, the band gap of the perovskite film can be calculated using Tauc's equation:***

$$\alpha h\nu = B(h\nu - E_g)^n \quad (\text{Eq. S1})$$

where h is the Planck constant, ν is the frequency of the light, α is absorption coefficient, B is the constant, which should be 1 here, E_g is the energy gap of the perovskite, and n is the index (values of 1/2 correspond to direct allowed). The Tauc plots of the TCP film were constructed in the inset of Fig. S1a, the value of the band gap is calculated to be 1.59 eV by finding the maximum value of E_g at $(\alpha h\nu)^2=0$.

X-ray photoelectron spectroscopy (XPS) spectrum is illustrated in Fig. S1b, the energy positions in the survey spectrum are proved to be I4d (49 eV), Br3d (68 eV), Pb4f (138 eV), C1s (284 eV), Pb4d (413 eV), I3d (619 eV), and Cs3d (724 eV), respectively. For some elements, there are two Gaussian peaks, which is due to the spin polarization.

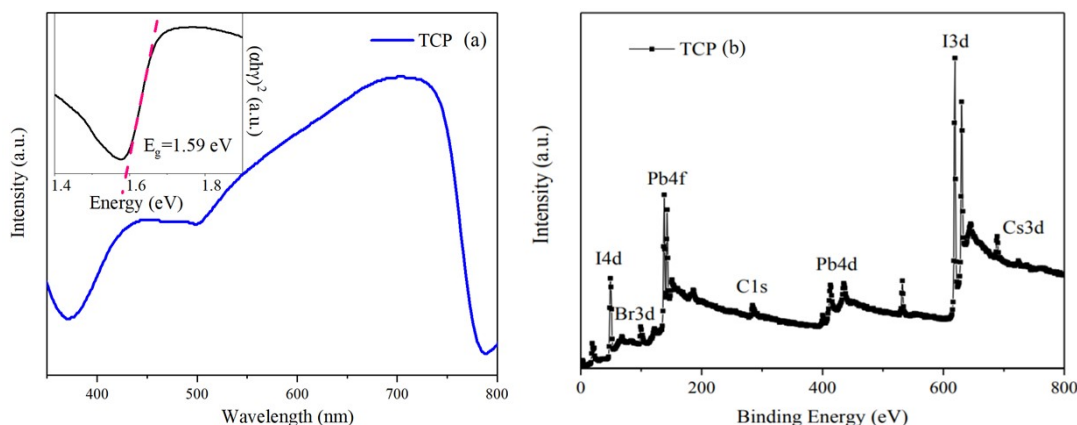


Fig. S1 (a) UV-vis absorption spectrum and the Tauc plot for band gap calculation (Inset) of the triple cation perovskite (TCP). (b) X-ray photoelectron spectroscopy spectrum of TCP.

X-ray diffraction (XRD) spectrum of triple cation organic-inorganic hybrid perovskite (TCP) film is illustrated in Fig. S2. The crystalline phase of the original perovskite is detected by containing the diffractions for (100), (110), (111), (200), (210), and (220) planes, which is assigned to the cubic structure of the $CS_{0.05}(FA_xMA_{1-x})_{0.95}PbI_yBr_{3-y}$ films.

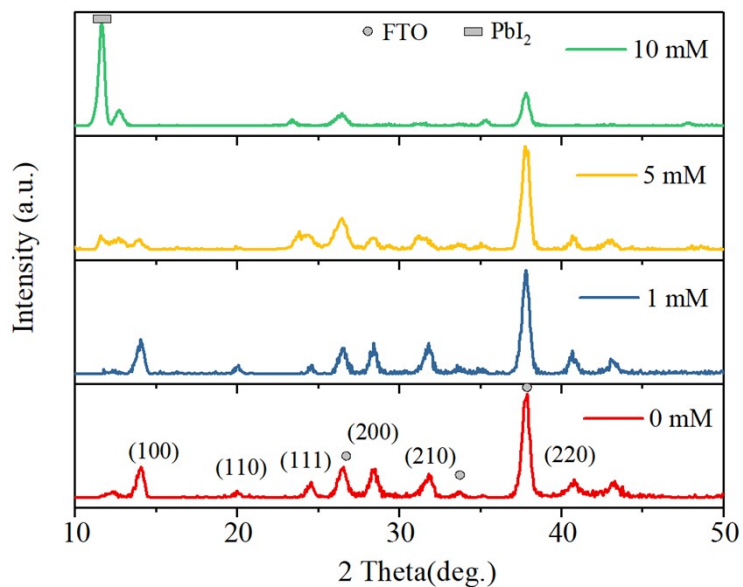


Fig. S2 X-ray diffraction spectrum of CsMAFAPbI₂Br film with various iodine concentrations (0, 1, 5, 10 mM)

The high resolution surface morphologies were characterized by SEM measurements and shown in Fig. S3.

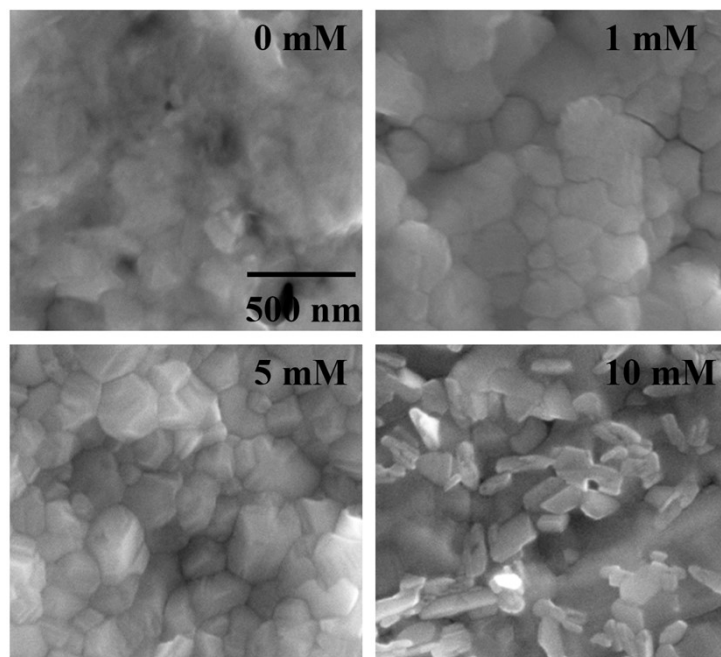


Fig. S3 Field emission scanning electron images of perovskite films with various ion concentrations (0, 1, 5 and 10 mM)

The repeated current-voltage (I-V) curves with various ion concentrations are given in Fig. S4.

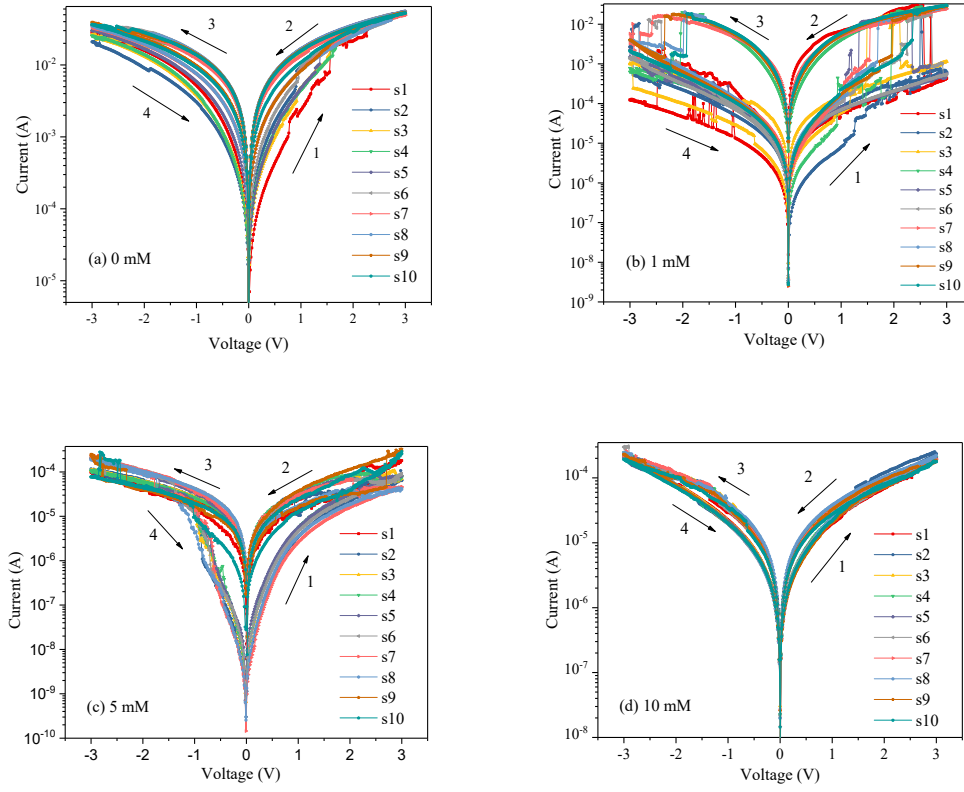
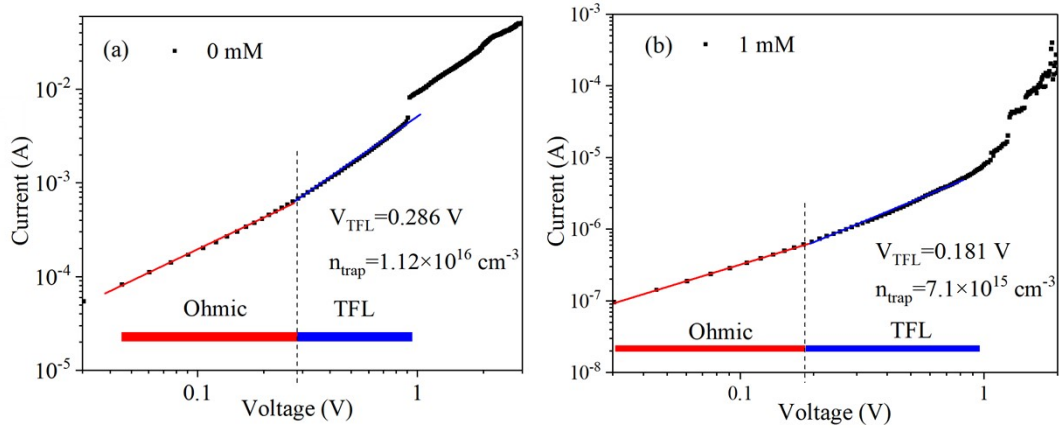


Fig. S4 Current-voltage sweeping curves (10 cycles) of perovskite memristors with (a)0, (b)1, (c)5, and (d)10 mM ion concentrations, respectively.

The concentration of the traps in the perovskite film can be characterized by space-charge-limited current analysis and shown in Fig. S5. The trap density N_{trap} is calculated by the following equation:

$$N_{trap} = \frac{2\varepsilon_0\varepsilon_r V_{TFL}}{eL^2} \quad (\text{Eq. S2})$$

where ε_0 is the vacuum permittivity, ε_r is the relative dielectric constant of TCP, V_{TFL} is the trap-filled limit voltage, e is the electron charge, and L is the thickness of TCP.



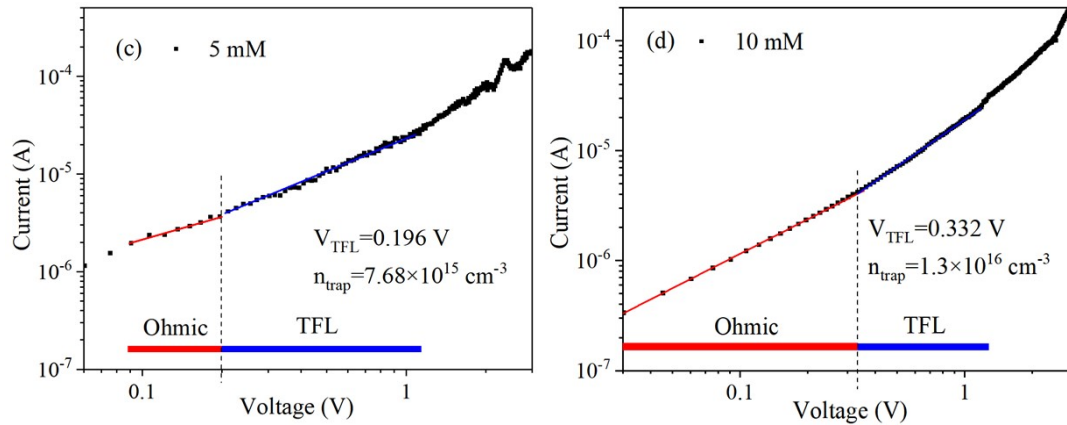


Fig. S5 Space-charge limited current measurements for the memristors with various iodine concentrations (a) 0 mM; (b) 1 mM; (c) 5 mM; (d) 10 mM.

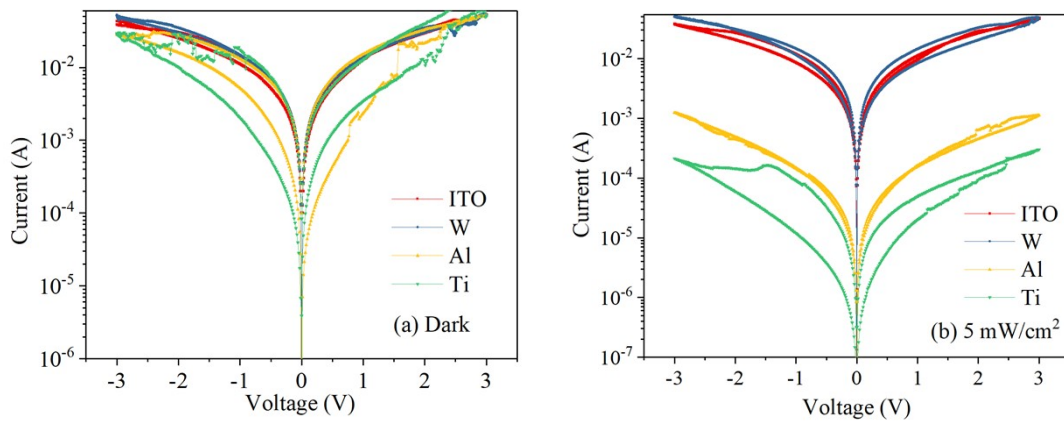


Fig. S6. Current-Voltage curves of the perovskite based memristors with various electrodes (ITO, W, Al, and Ti) under (a) Dark; (b) 5 mW/cm².

Current-Voltage curves of FTO/TCP/Metal memristors with various electrodes (ITO, W, Al, and Ti) under different light conditions are illustrated in Fig. S6. For the inert electrodes (ITO and W), the hysteresis loops are quite small and the current values do not change when 5 mW/cm² light source is applied. However, the active electrodes (Al and Ti) present different results. Both the current loops and values are reduced by stimulation of light.

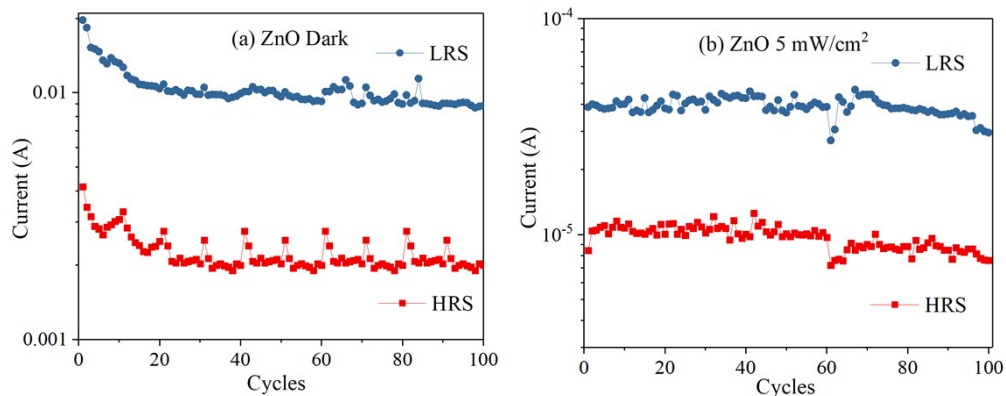


Fig. S7. Endurance performance of the FTO/ZnO/TCP/Ti memristors. Switching between HRS (red, 0.5 V) and LRS state (blue, -2.5 V) under (a) Dark; (b) 5 mW/cm².

Endurance performance of the FTO/ ZnO/TCP/Ti memristors under dark and 5 mW/cm² conditions are shown in Fig. S7, indicating that the device can stably change between high resistance state (HRS) and low resistance state (LRS) for 100 reversible cycles.

The structure diagram of FTO/TCP/P3HT/Au memristor is shown in Fig. S8a, and repeated I-V curves under various light conditions are given in Fig. S8b and c. The curves show good stability and consistency, without serious current fluctuation and zero drift effect. This proves that the interface of our perovskite is greatly modified and the film traps are reduced. When it occurs to Fig. S8b and c, the hysteresis loops are largely reduced after illumination, which means the iodine vacancy migration no longer accounts for the main role in memristor mechanism. However, light injection has almost no impact on the current values, this may be because the P3HT layer blocks most illumination.

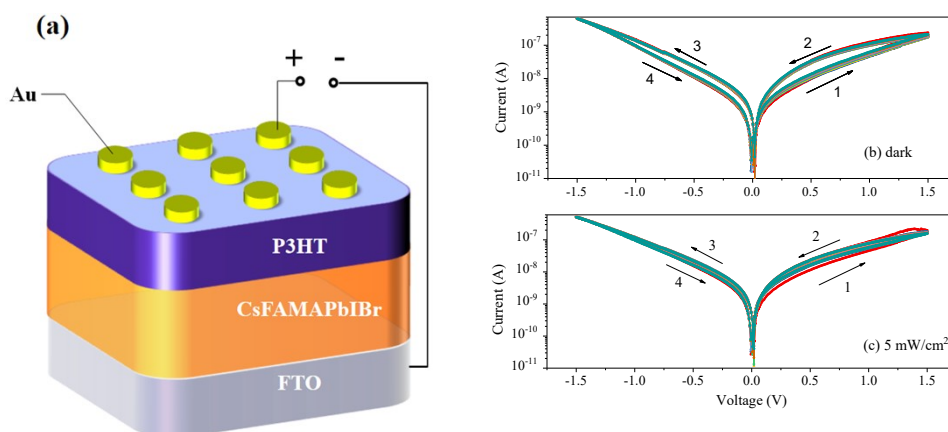


Fig. S8 (a) Structure diagram of FTO/perovskite/P3HT/Au memristor. Repeated Current-Voltage curves under (b) dark and (c) 5 mW/cm².

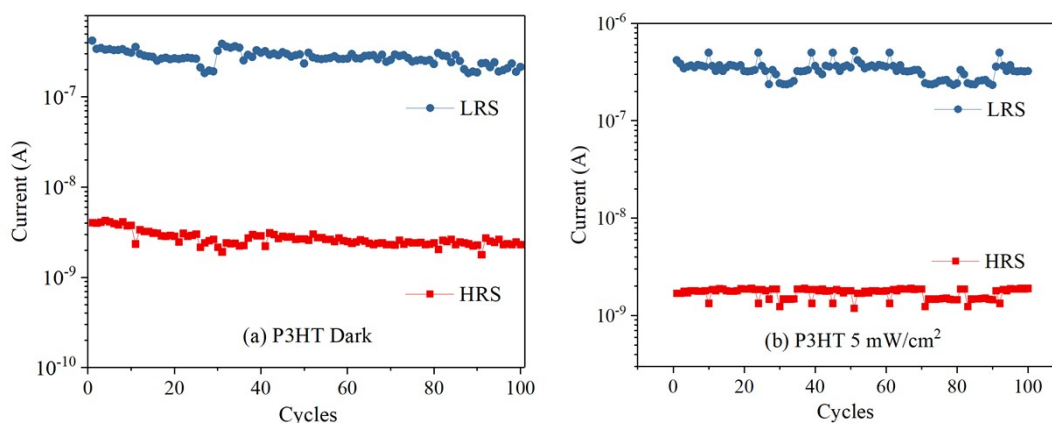


Fig. S9. Endurance performance of the FTO/TCP/P3HT/Ti memristors. Switching between HRS (red, 0.2 V) and LRS state (blue, -1.3 V) under (a) Dark; (b) 5 mW/cm².

Endurance performance of the FTO/TCP/P3HT/Ti memristors under dark and 5 mW/cm² conditions are shown in Fig. S9, indicating that the device can stably change between high resistance state (HRS) and low resistance state (LRS) for 100 reversible cycles.

Table S1. Characteristics of perovskite memristors under different ion concentrations, electrode types and modified layers

Condition	Iodine concentration				Electrode Type (Dark:D, Light:L)				Modified Layer	
					Inert Electrode		Active Electrode			
	0 mM	1 mM	5 mM	10 mM	ITO	W	Al	Ti	ZnO	P3HT
Trap Density (cm ⁻³)	1.1×10 ¹⁶	7.1×10 ¹⁵	7.7×10 ¹⁵	1.3×10 ¹⁶	-	-	-	-	-	-
Maximum HRS/LRS ratio	10.83	130.5	82	-	-	-	D:23 L:1.4	D:17.5 L:5.2	-	-
Current Values (A, 1 V, HRS)	5.4×10 ⁻³	2.8×10 ⁻⁵	3.6×10 ⁻⁶	2.6×10 ⁻⁵	D:1.4×10 ⁻² L:1×10 ⁻²	D:1.5×10 ⁻² L:9.7×10 ⁻³	D:2.3×10 ⁻³ L:1.6×10 ⁻⁴	D:3.4×10 ⁻³ L:3×10 ⁻⁵	D:3.2×10 ⁻³ L: 2.5×10 ⁻⁵	D:3×10 ⁻⁸ L: 3×10 ⁻⁸
Current Switching Type	Analog	Digital	Digital-Analog	Analog	D:Analog L:Analog	D:Analog L:Analog	D:Digital-Analog L: Analog	D:Digital-Analog L: Digital-Analog	D:Analog L:Analog	D:Analog L:Analog
Endurance	-	-	-	-	-	-	-	-	100	100

Characteristics of perovskite memristors under different ion concentrations, electrode types and modified layers are summarized in Tab. S1.